

See discussions, stats, and author profiles for this publication at: <https://www.researchgate.net/publication/255983060>

Water-Soluble Conjugated Polymers for Simultaneous Two-Photon Cell Imaging and Two-Photon Photodynamic Therapy

ARTICLE *in* ADVANCED OPTICAL MATERIALS · JANUARY 2013

Impact Factor: 4.06 · DOI: 10.1002/adom.201200026

CITATIONS

12

READS

86

6 AUTHORS, INCLUDING:



Xiaoqin Shen

University of California, Santa Barbara

12 PUBLICATIONS 261 CITATIONS

SEE PROFILE



Shao Q Yao

National University of Singapore

190 PUBLICATIONS 5,081 CITATIONS

SEE PROFILE



Qing-Hua Xu

National University of Singapore

129 PUBLICATIONS 3,228 CITATIONS

SEE PROFILE

Water-Soluble Conjugated Polymers for Simultaneous Two-Photon Cell Imaging and Two-Photon Photodynamic Therapy

Xiaoqin Shen, Lin Li, Agnes Chow Min Chan, Nengyue Gao, Shao Q. Yao, and Qing-Hua Xu*

Conventional photosensitizers generally suffer from low efficiency in novel non-invasive two-photon photodynamic cancer therapy due to their small two-photon absorption cross section and they lack an imaging capability for therapy guiding due to their low fluorescence yield. Demonstrated here is the first water-soluble conjugated polymers as direct two-photon photosensitizers with dual capability of two-photon cell imaging and two-photon photodynamic therapy. By introducing a strong electron-withdrawing cyano group into the phenyl ring of the backbone, the cyano-substituted poly(fluorene-2,7-ylenevinylene-co-phenylene) (PFVCN) displays a 2.4 times higher maximum two-photon absorption cross section per repeat unit and significantly higher fluorescence quantum yield in water than the unsubstituted PFV. The large two-photon absorption cross section of PFVCN allows it to efficiently generate singlet oxygen under two-photon excitation, which is critical for two-photon photodynamic therapy. Two-photon excitation cell imaging and efficient two-photon-induced photodynamic therapy effect on cancer cells of PFVCN are successfully demonstrated. These studies provide insight in designing novel photosensitizing agents for simultaneous two-photon imaging and two-photon photodynamic therapy, which allows two-photon imaging guided therapy to fully take the unique advantages of two-photon excitation such as deep penetration and 3D selectivity.

the light for two-photon excitation falls into biological tissue transparency window (700–1000 nm), which can penetrate deeper into diseased tissues. Secondly, it allows working with a smaller, more confined treatment area. Most importantly, it renders selective activity in z-direction, which allows 3D selectivity and thus significantly reduces side effects. The key prerequisite for two-photon PDT is photosensitizers that can efficiently generate singlet oxygen under two-photon excitation.^[3] However, most photosensitizers in clinical use have been optimized for the conventional one-photon PDT and have very small two-photon absorption (TPA) cross sections. Their efficiencies for two-photon PDT are generally low.^[4] To make two-photon PDT more widely applicable, lots of efforts have been made to synthesize new photosensitizers with large TPA cross sections,^[5] or improve two-photon properties of traditional photosensitizers via energy transfer from materials with large TPA cross sections.^[6]

Imaging is crucial for diagnosing diseases, guiding and monitoring the treatment as well as following up to assess the success of the therapy

Imaging guided therapy is an excellent method for both localizing cancer targets during treatment and monitoring the treatment outcome invasively. Integration of fluorescence imaging with PDT has been successfully used in preclinical studies.^[8] However, to use the conventional photosensitizers as both therapeutic and imaging agents, excitation in the UV-Visible range is generally used to generate fluorescence emission. This approach suffers from limited tissue penetration depth and strong auto-fluorescence background of biological tissues. Two-photon imaging has been widely recognized as a noninvasive diagnostic technique.^[9] The combination of two-photon imaging with two-photon PDT has many unique advantages.^[4,7] It is of great interest to develop effective two-photon photosensitizers for simultaneous two-photon imaging and PDT.^[5a,10]

Water soluble conjugated polymers have found a lot of biological applications due to their large extinction coefficients, high fluorescence quantum yield and fluorescence amplification of small molecules through energy transfer.^[11] Water

1. Introduction

A long-standing dream in the field of cancer therapy is to treat subcutaneous tumors noninvasively while at the same time eliminating the adverse physical discomfort associated with traditional chemotherapy and debilitating effect of actinic radiation treatments.^[1] Two-photon photodynamic therapy (PDT) is a promising noninvasive treatment of cancers and other diseases.^[2] Two-photon PDT is advantageous over the traditional one-photon counterpart in a few aspects. First, wavelength of

X. Q. Shen, Dr. L. Li, A. C. M. Chan, N. Y. Gao,
Prof. S. Q. Yao, Prof. Q.-H. Xu
Department of Chemistry
National University of Singapore
3 Science Drive 3, 117543, Singapore
E-mail: chmxqh@nus.edu.sg



DOI: 10.1002/adom.201200026

soluble conjugated polymers have also been found to display large TPA cross section and have been utilized as two-photon light harvesting materials to enhance two-photon emission of photosensitizers by energy transfer processes.^[12,13] Conjugated polymer nanoparticles contain tens of polymer chains with large TPA across section per particle^[14a] and have been demonstrated to act as long-term intracellular probe for two-photon imaging due to their low cytotoxicity compared with quantum dots.^[14b,c] So far, the TPA cross sections of the conjugated polymers are still relatively low, ranging from tens to ~250 GM per repeat unit at 800 nm, which have large room to be further improved. Although water soluble conjugated polymers have been reported to generate singlet oxygen under one-photon excitation,^[15,16] there is no report on direct singlet oxygen generation by water soluble conjugated polymers under two-photon excitation. We recently reported that polyfluorene-vinylene type conjugated polymer have larger TPA cross section compared to polyfluorene-ethylene type.^[12c] Thus, it would be of great interest to investigate two-photon induced singlet oxygen generation efficiency of water soluble conjugated polymers and their applications as two-photon excitation photosensitizers for potential applications in simultaneous two-photon PDT and two-photon imaging, which allows imaging guided therapy.

In this contribution, we synthesized a series of polyfluorene-vinylene-phenylene type water soluble conjugated polymers by introducing different substitution groups into the backbone. Electron donating methoxy group or electron withdrawing cyano group was introduced into the phenyl ring of conjugated polymer backbone for poly[9,9-bis(6''-(*N,N,N*-trimethylammonium) fluorene-2,7-ylenevinylene-*co*-alt-1,4-(2,5-dimethoxyphenylene)] (PFVMO) and poly[9,9-bis(6''-(*N,N,N*-trimethylammonium)hexyl)fluorene-2,7-ylenevinylene-*co*-alt-1,4-(2,5-dicyanophenylene)] (PFVCN). The one- and two-photon optical properties of these water soluble conjugated polymers have been investigated. Among three polymers, PFVCN was found to display high fluorescence quantum yield and much larger two-photon (TP) action cross section than PFVMO and the un-substituted PFV. Singlet oxygen generation by these polymers under two-photon excitation has also been evaluated. The application of PFVCN as highly bright two-photon excitation

cell imaging agent with efficient two-photon induced photodynamic therapy effect on cancer cells have been successfully demonstrated.

2. Results and Discussion

2.1. Synthesis of Three Conjugated Polymers

The synthetic procedures of three conjugated polymers are shown in **Figure 1**. Poly[9,9-bis(6''-(bromohexyl)fluorene-2,7-ylenevinylene-*co*-alt-1,4-phenylene] (PFV-Br), poly[9,9-bis(6''-(bromohexyl)fluorene-2,7-ylenevinylene-*co*-alt-1,4-(2,5-dimethoxyphenylene)] (PFVMO-Br) and poly[9,9-bis(6''-(bromohexyl)fluorene-2,7-ylenevinylene-*co*-alt-1,4-(2,5-dicyanophenylene)] (PFVCN-Br) were synthesized by using a previously reported method via the Wittig-Horner condensation reaction between dialdehyde and 1,4-bis(diethylphosphina tilmethyl) phenylene in dry tetrahydrofuran (THF) by slowly adding 1 equiv of *t*-BuOK.^[12c] Water soluble cationic conjugated polymers PFV, PFVMO and PFVCN were obtained by quaternization of the neutral polymers PFV-Br, PFVMO-Br and PFVCN-Br in excess of trimethylammonium in methanol/chloroform at room temperature for 48 h. The molecular weights of the neutral polymers were determined by gel permeation chromatography (GPC) using THF as the eluent. The number-averaged molecular weights (*M_n*) for PFV-Br, PFVMO-Br, and PFVCN-Br were determined to be 17100 with PDI (*M_w*/*M_n*) = 1.81, 19200 with PDI = 2.12, and 10100 with PDI = 1.98, respectively. The numbers of repeat unit for PFV-Br, PFVMO-Br, and PFVCN-Br are 28, 29, and 15, respectively. The polydispersity properties of the polymers are summarized in **Table 1**.

2.2. One- and Two-photon Optical Properties of the Polymers

The one-photon optical properties of three water soluble conjugated polymers in aqueous solution are shown in **Figure 2**. The absorption maxima of PFV, PFVMO and PFVCN are located

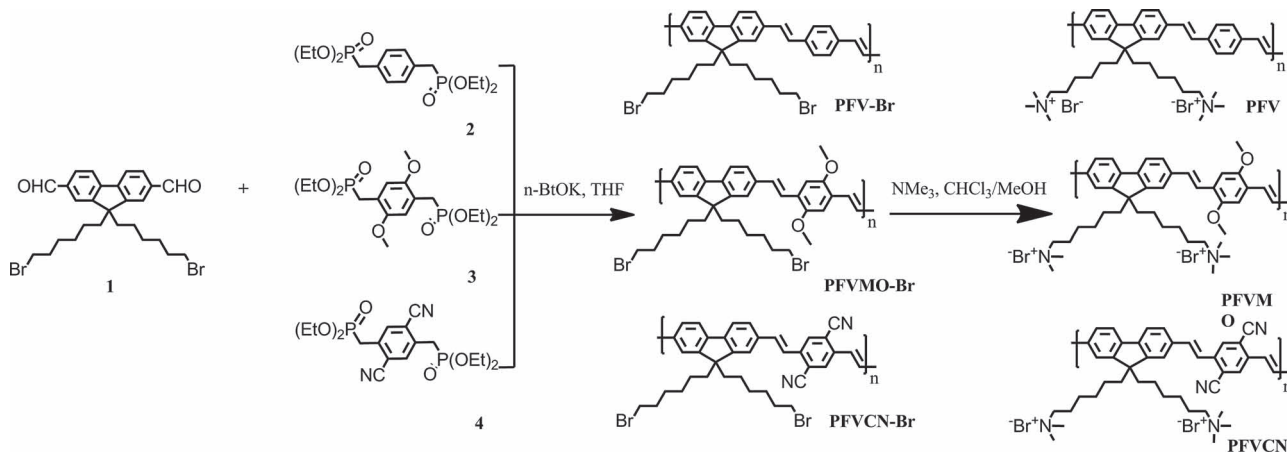


Figure 1. Synthesis procedures of three conjugated polymers.

Table 1. Polydispersity properties of the conjugated polymers.

Polymer	M_n [g mol ⁻¹]	PDI	Number of repeat units
PFV-Br	17100	1.81	28
PFVMO-Br	19200	2.12	29
PFVCN-Br	10100	1.98	15

at 435, 451, and 469 nm, while the corresponding emission maxima are located at 483, 510, and 556 nm, respectively. The absorption and emission spectra of PFVMO and PFVCN are red-shifted relative to those of PFV. The red-shift of absorption and emission maxima from PFV to PFVMO and PFVCN can be ascribed to introduction of electron donating methoxy group and electron withdrawing cyano group in the conjugated backbone that extend the conjugation length.^[17]

The quantum yields (QYs) of PFV, PFVMO and PFVCN were measured to 1.8%, 1.5%, and 20% in water, and 33%, 28% and 42% in methanol, respectively. Cationic conjugated polymers generally display low emission efficiency in water due to formation of aggregates driven by the highly hydrophobic conjugated backbone and aggregation-induced quenching of intrachain singlet excitation.^[18] It is interesting to note that QY of PFVCN is still relatively high (20%). A few water soluble conjugated polymers were previously reported to display reasonably high QY in water, which was ascribed to the formation of excimer-like state via interchain interactions.^[18b,19] Substitution of electron withdrawing cyano groups in an aromatic hydrocarbons can promote formation of DA-like exciplex through interactions with other aromatic hydrocarbons (acting as electron donors).^[20] For PFVCN in water, aggregation promotes the formation of DA excimer-like state via the interchain interaction between the bicyano substituted benzene units with aromatic fluorene units (electron donors), resulting in a relatively high QY. In PFV and PFVMO, non-fluorescent (or very weakly fluorescent) aggregates formed, which act as an energy trap and lead to rapid quenching of the intrachain exciton and very low QY.^[18b,19] Lifetime measurements (See Figure S1 in the Supporting Information) reveal that PFV and PFVMO in water displayed very rapid overall fluorescence

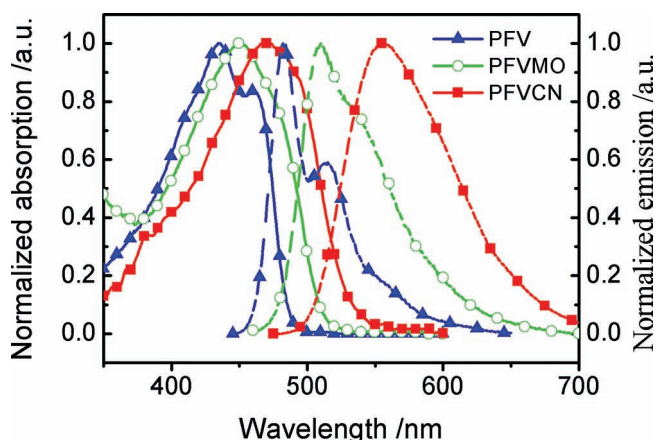


Figure 2. Normalized absorption (solid lines) and fluorescence spectra (dashed lines) of PFV, PFVMO, and PFVCN in water.

decay, much faster than those in methanol, consistent with their low QYs in water. In contrast, the overall decay for PFVCN in water is slower than that in MeOH. This results suggest the formation of an “excimer-like” state, which has a longer radiative decay compared to an intrachain singlet exciton.^[18] The concentration dependence of fluorescence spectra of and wavelength dependence of time-resolved spectra PFVCN in water (10% MeOH) further confirm the formation of excimer-like aggregates (See Figure S2 in the Supporting Information). The high fluorescence QY of PFVCN is advantageous for its applications in bio-imaging. Dynamic light scattering (DLS) measurement (See Figure S3 in the Supporting Information) shows that the average particle size of three conjugated polymer aggregates are 32, 27, and 122 nm, for PFV, PFVMO and PFVCN, respectively, which are in the range for efficient cell uptake.^[21]

Two-photon excitation properties of the cationic polymers PFV, PFVMO, and PFVCN were measured by using femtosecond laser pulses from 750 to 850 nm (Figure 3a). The

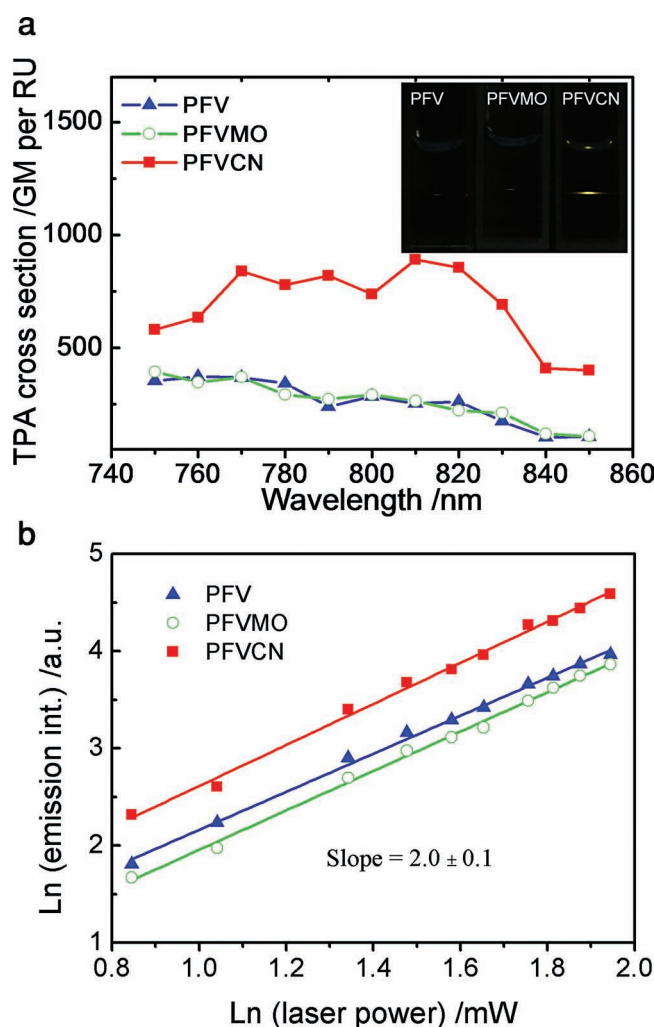


Figure 3. (a) Two-photon excitation spectra of PFV, PFVMO, and PFVCN in water. The TPA cross section values were calculated base on per repeat unit of the polymers (GM per RU). The inset shows their photographs under fs laser excitation at 810 nm. (b) Excitation power dependence of fluorescence intensity under excitation at 810 nm.

two-photon excitation nature was confirmed by excitation intensity dependent fluorescence intensity of the polymers under excitation at 810 nm. The log-log plots (Figure 3b) give slopes of 2.0 ± 0.1 for all three polymers. The quadratic dependence of their emission intensities on excitation power confirms that the observed emission indeed arises from two-photon excitation. The maximum TPA cross section was located at ~ 760 nm for PFV and PFVMO, and 810 nm for PFVCN. This is important for practical applications because the central wavelength of the most readily available femtosecond laser source is located at ~ 800 nm. The maximum TPA cross section value per repeat unit reached 370 GM for PFV, 390 GM for PFVMO, and 891 GM for PFVCN, respectively. The TPA cross section per repeat unit has been enhanced by ~ 2.4 folds by introducing strong electron withdrawing cyano group into phenyl ring of the backbone. This result is consistent with the previous studies on cyano-substituted conjugated small molecules,^[17] which is ascribed to increased conjugation length due to electron withdrawing effects of cyano group and less degree of distortion from planarity.

TPA action cross section ($\phi\delta$) is usually used to evaluate the brightness of two-photon fluorophores, where δ is the TPA cross section and ϕ is the fluorescence quantum yield.^[22] So far a few reported water soluble chromophores showed TPA action cross section values ranging from 10 to 700 GM in water in the non-aggregated form.^[23] The TPA action cross section values of the prepared PFV, PFVMO, and PFVCN were calculated to be 4.55 GM, 3.97 GM, and 179 GM per repeat unit. In practical applications, TPA action cross value is generally calculated based on a molecule or a nanoparticle containing several molecules.^[11b,14b] The TPA action cross values based on a molecule were calculated to be 128 GM, 115 GM, and 2673 GM per molecule for PFV, PFVMO, and PFVCN (Table 2). The two-photon excitation fluorescence of PFVCN can be even directly visualized with naked eyes (Figure 3a inset) due to its high TPA action cross section. These water soluble conjugated polymers are expected to display high brightness in two-photon imaging applications.

2.3. Dark Cytotoxicity of the Polymers

Good biocompatibility and low dark cytotoxicity are essential for any chromophore in biological applications such as bioimaging and phototherapy. The cytotoxicity of three water soluble conjugated polymers in dark was evaluated by monitoring the metabolic viability of HeLa cells. Figure 4 shows the cell

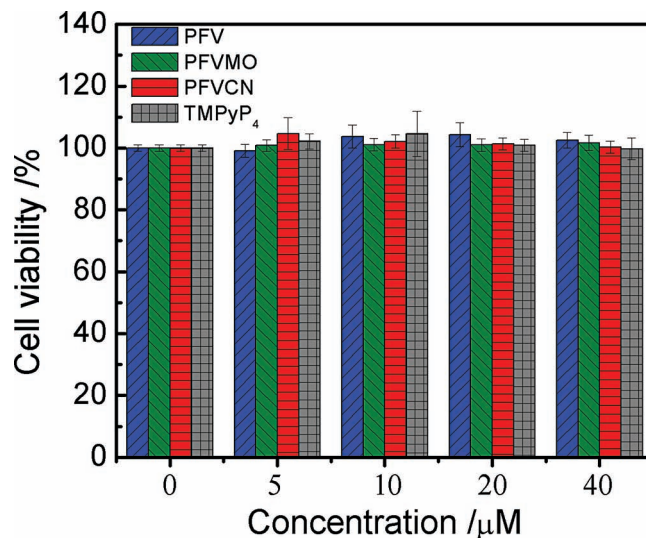


Figure 4. Metabolic viability of HeLa cells after incubation with PFV, PFVMO, PFVCN and TMPyP₄ of different concentrations (in repeat unit for polymers) for 24 h.

viability after incubation with PFV, PFVMO, PFVCN, and TMPyP₄ at different concentrations for 24 h in dark. The metabolic viability of the cells remained nearly 100% when the concentrations of polymers reached up to 40 μM . The low dark cytotoxicity of the polymers ensures their applications in real practice.

2.4. Two-photon Excitation Cell Imaging

The large TPA action cross sections of these conjugated polymers, in particular PFVCN, make them attractive candidates for two-photon imaging agents. Two-photon excitation cell imaging using PFV, PFVMO, PFVCN, and TMPyP₄ were demonstrated by using HeLa cancer cells under excitation at 810 nm using a two-photon laser scanning confocal microscopy (Figure 5). Intense fluorescence signals were observed from the cells treated with PFVCN, while relatively weak fluorescence signals were observed from cells treated with PFV and PFVMO under identical experimental conditions, which is consistent with their relative TPA actions cross section values. No fluorescence signal was observed from cells treated with TMPyP₄ as expected, due to its low quantum yield and small TPA cross section. Overlaid pictures of the two-photon

Table 2. Photophysical properties of the conjugated polymers in comparison with TMPyP₄.

Compd	λ_{abs} [nm]	ϵ [M ⁻¹ cm ⁻¹]	λ_{em} [nm]	ϕ [%] ^{a)}	δ [GM] ^{b)}	$\phi\delta$ [GM] ^{c)}	δ [GM] ^{d)}	$\phi\delta$ [GM] ^{e)}
PFV	435	2.43×10^4	483	1.8	253	4.55	7084	128
PFVMO	451	1.31×10^4	510	1.5	265	3.97	7685	115
PFVCN	469	1.48×10^4	556	20	891	179	13365	2673
TMPyP ₄	421	24.0×10^4	657	0.3	10	0.03	10	0.03

^{a)}Measured in water solutions, fluorescein in NaOH water solution (PH = 11) was used as a standard for quantum yield measurements; ^{b)}TPA cross section per repeat unit at 810 nm; ^{c)}Two-photon action cross section per repeat unit at 810 nm; ^{d)}TPA cross section per molecule; ^{e)}Two-photon action cross section per molecule.

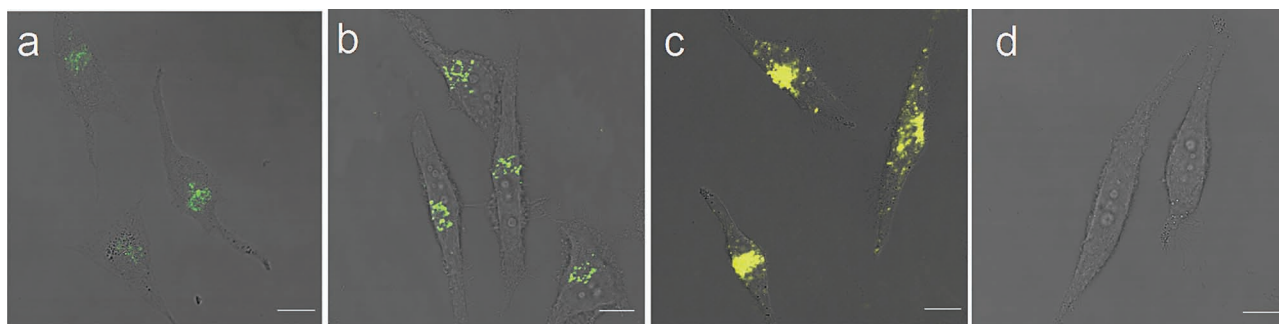


Figure 5. Overlaid images of two-photon excitation fluorescence and bright field images of HeLa cancer cells treated with PFV (a), PFVMO (b), PFVCN (c), and TMPyP₄ (d) for 3 h. Scale bar: 10 μ m.

excitation fluorescence images and bright field images show that these polymers were successfully taken up and internalized into the cells after incubation for 3 hours. These results indicate that these water soluble polymers, in particular PFVCN, can act as promising agents for two-photon cell imaging with high brightness.

2.5. Singlet Oxygen Generation

Singlet oxygen is responsible for killing cancer cells in PDT. High singlet oxygen generation efficiency is required for the application of photosensitizers in PDT. Some water soluble conjugated polymers are known to generate singlet oxygen and could also be used as photosensitizers.^[15c,15d] Singlet oxygen generation efficiencies of PFV, PFVMO and PFVCN were examined by monitoring the characteristic emission peak of singlet oxygen at ~ 1270 nm in CD₃OD solution. Under excitation at their corresponding absorption maxima, three polymers all displayed the characteristic singlet oxygen emission band at ~ 1270 nm (Figure 6a), which disappeared in oxygen deficient solution by bubbling with N₂ gas for about 15 min (see Figure S4 in the Supporting Information). This result confirms that the observed emission peak indeed originates from singlet oxygen generated from the interaction between the polymers and molecular oxygen. Using TMPyP₄ in D₂O as standard, the singlet oxygen generation yields were calculated to be 5.6%, 4.3%, and 6.9% for PFV, PFVMO, and PFVCN, respectively.

Two-photon induced singlet oxygen generation of the polymers in water was evaluated by a chemical method using 1,3-cyclohexadiene-1,4-diethanoate (CHDDE) as a probe. In this method, CHDDE reacts with singlet oxygen to form peroxide and hydroperoxide, leading a decrease in its absorption band at 270 nm.^[24] The UV absorption at 270 nm was monitored during the course of irradiation by femtosecond laser pulses at 810 nm in the presence of polymers. The control experiments were done in the presence of TMPyP₄ under the same experimental conditions. As shown in Figure 6b, the CHDDE photo-oxidation rate in the presence of PFVCN is significantly faster than that in the presence of PFV, PFVMO, and TMPyP₄. The trend is consistent with their two-photon induced singlet oxygen generation capability, which could be characterized by $\delta\Phi_{\Delta}$, the product of TPA cross section and singlet oxygen

generation efficiency. As shown in Table 3, $\delta\Phi_{\Delta}$ of PFVCN is 61 GM per repeat unit, ~ 8 times higher than that of TMPyP₄ (7.4). This result indicates that PFVCN can generate singlet oxygen

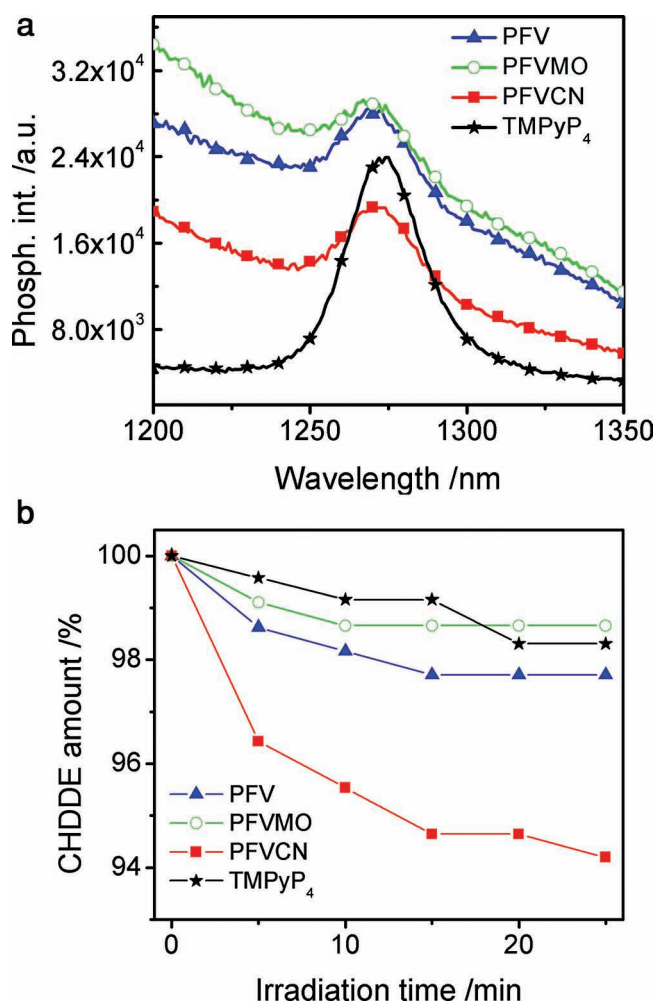


Figure 6. (a) Phosphorescence spectra of singlet oxygen generated by PFV, PFVMO, and PFVCN in CD₃OD under one-photon excitation. TMPyP₄ in D₂O was used as the standard. (b) Comparison of time dependent CHDDE degradation in presence of PFV, PFVMO, PFVCN and TMPyP₄ under two-photon excitation at 810 nm.

Table 3. Singlet oxygen generation efficiency of the conjugated polymers and TMPyP₄.

Compound	δ [GM] ^{a)}	Φ_{Δ} [%] ^{b)}	$\delta\Phi_{\Delta}$
PFV	253	5.6	14
PFVMO	265	4.3	11
PFVCN	891	6.9	61
TMPyP ₄	10	74 ^{c)}	7.4

^{a)}TPA cross section per repeat unit at 810 nm; ^{b)}Singlet oxygen generation yield Φ_{Δ} was calculated based on the singlet oxygen luminescence intensity at ~1270 nm, using TMPyP₄ as the standard; ^{c)}Value taken from Ref. [3d].

under two-photon excitation with high efficiency and thus can be utilized as photosensitizers for two-photon PDT.

2.6. Two-photon Induced Cytotoxicity

Since PFVCN display much larger $\delta\Phi_{\Delta}$ compared to PFV, PFVMO and TMPyP₄, we further explored its potential application as a two-photon PDT photosensitizing agent. The viability of Hela cancer cells incubated with PFVCN or without PFVCN were examined after exposure to femtosecond laser irradiation at 810 nm with energy density of ~3.0 W cm⁻². The laser beam was unfocused with a beam size of ~0.3 cm². The final concentration of PFVCN was 20 μ M (in repeat unit). For direct comparison, the experiments on cells treated with TMPyP₄ of the same concentration were also performed under the same experimental conditions. **Figure 7** shows irradiation time dependent cell viability of Hela cancer cells after two-photon photodynamic treatment. The viability of the cells without PFVCN was found to remain nearly 100% under

laser irradiation for 10 min, indicating that the cells were not directly killed by the laser irradiation. In contrast, the viability of the cells treated with PFVCN showed dramatically decrease with the increasing laser irradiation time. The cell viability decreased to ~46% when the irradiation time reached 10 min. In comparison, the viability of the cells treated with TMPyP₄ showed no obvious change under the same condition, consistent with the much smaller TPA cross section of TMPyP₄. These results indicate that PFVCN can act as efficient photosensitizers for two-photon photodynamic treatment on cancer cells, owing to its large TPA cross section and capability of singlet oxygen generation ($\delta\Phi_{\Delta}$).

3. Conclusion

In summary, we have developed water soluble conjugated polymers with large TPA cross sections for simultaneous two-photon cell imaging and two-photon PDT. Three different water soluble conjugated polymers, poly(fluorene-2,7-ylenevinylene-co-phenylene) with different substitution groups on the backbone, have been synthesized. By introducing strong electron withdrawing cyano group into phenyl ring of the backbone, PFVCN displayed 2.4 time higher maximum TPA cross section per repeat unit and significantly higher fluorescence quantum yield (~20%) in water than the unsubstituted PFV. The two-photon action cross section of PFVCN is 39 times higher than that of PFV at 810 nm. The large two-photon action cross section of PFVCN makes it a promising material for two-photon cell imaging. Moreover, PFVCN displayed high two-photon induced singlet oxygen generation activity due to its large TPA cross section and reasonable singlet oxygen generation yield. The two-photon PDT effect of PFVCN on cancer cells was found to be much higher than porphyrin type photosensitizer, TMPyP₄. These studies suggest that water soluble conjugated polymers can be developed as promising novel photosensitizing agents with dual capability of two-photon imaging and two-photon PDT, which allows two-photon imaging guided therapy.

4. Experimental Section

Materials: Solvents and chemicals were purchased from Sigma-Aldrich and used as received without further purification unless otherwise noted. Dulbecco's modified eagle medium (DMEM), fetal bovine serum, streptomycin, and penicillin were purchased from Invitrogen. THF was dried and distilled under sodium. 2,7-Diformyl-9,9-di(6'-bromohexyl) fluorene (1),^[12c] 1,4-bis(diethyl phosphinanyl methyl)benzene (2),^[17a] 1,4-bis(diethyl phosphinanyl methyl)-2,5-dimethoxybenzene (3),^[25a] 1,4-bis(diethylphosphinanyl methyl)-2,5-dicyanobenzene (4),^[25b] and 1,3-cyclohexadiene 1,4-diethanoate (CHDDE)^[24] were prepared according to the reported procedures.

Synthesis of the Neutral Conjugated Polymers: A solution of phosphonate (2, 3, or 4) (0.5 mmol) and monomer 1 (0.5 mmol) in dry THF (20 mL) was stirred at room temperature. After potassium tert-butoxide (2 mmol) was slowly added, the solution was stirred for 4 h at room temperature before being quenched with dilute aqueous HCl (20 mL). The solution was then poured into methanol (250 mL) under stirring. The precipitate was collected by filtration. The crude polymer was dissolved in THF, precipitated in methanol three times, and then dried under vacuum to give solid product.

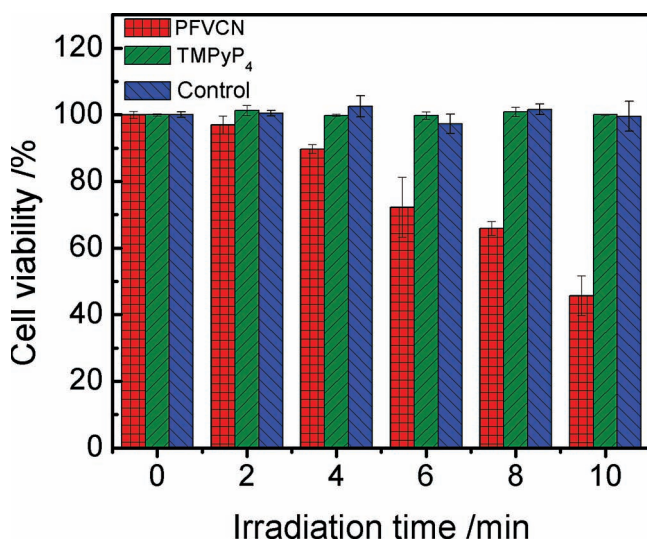


Figure 7. Laser irradiation time dependent cell viability of Hela cancer cells treated with PFVCN and TMPyP₄ after two-photon PDT treatment (irradiation by femtosecond laser pulses at 810 nm). Experiments on cells without any photosensitizers were performed under the same irradiation condition as the control.

Poly[9,9-bis(6''-(bromohexyl)fluorene-2,7-ylenevinylene-co-alt-1,4-phenylene] (PFV-Br): Pure PFV-Br was obtained in 32% yield as a yellow solid. ¹H NMR (300MHz, CDCl₃, δ): 7.69 (br, 2H), 7.58–7.49 (br, 8H), 6.98 (s, 4H), 3.28 (br, 4H), 2.10 (br, 4H), 1.65–1.58 (br, 4H), 1.18–1.09 (br, 8H), 0.68–0.53 (br, 4H); GPC: Mn = 17100, Mw = 30965, PDI = 1.81.

Poly[9,9-bis(6''-(bromohexyl)fluorene-2,7-ylenevinylene-co-alt-1,4-(2,5-dimethoxyphenylene)](PFVMO-Br): Pure PFVMO-Br was obtained in 41% yield as a yellow solid. ¹H NMR (300MHz, CDCl₃, δ): 7.82–7.37 (m, 14H), 3.88 (br, 6H), 3.28 (br, 4H), 2.10 (br, 4H), 1.65–1.58 (br, 4H), 1.18–1.09 (br, 8H), 0.68–0.53 (br, 4H); GPC: Mn = 19200, Mw = 40714, PDI = 2.12.

Poly[9,9-bis(6''-(bromohexyl)fluorene-2,7-ylenevinylene-co-alt-1,4-(2,5-dicyanophenylene)](PFVCN-Br): Pure PFVCN-Br was obtained in 30% yield as an orange solid. ¹H NMR (300MHz, CDCl₃, δ): 7.89–7.48 (m, 14H), 3.25 (br, 4H), 2.08 (br, 4H), 1.55 (br, 4H), 1.17–1.11 (br, 8H), 0.61 (br, 4H); GPC: Mn = 10100, Mw = 20010, PDI = 1.98.

Preparation of Ionic Polymers: PFV-Br, PFVMO-Br and PFVCN-Br were dissolved in chloroform (20 mL). Trimethylamine (5 mL, 30%) in ethanol was then added. The mixture was stirred for 48 h at room temperature. The solid products PFV, PFVMO and PFVCN were obtained after evaporation of the solvent at vacuum. (a) ¹H NMR (300MHz, DMSO-d₆, δ) for PFV: 8.09–7.27 (m, 14H), 3.18 (br, 18H), 2.95 (br, 4H), 1.45 (br, 4H), 1.26–1.05 (br, 8H), 0.54 (br, 4H). (b) ¹H NMR (300MHz, DMSO-d₆, δ) for PFVMO: 8.01–7.37 (m, 14H), 3.83 (s, 6H), 3.17 (br, 18H), 2.95 (br, 4H), 1.47 (br, 4H), 1.27–1.05 (br, 8H), 0.55 (br, 4H). (c) ¹H NMR (300MHz, DMSO-d₆, δ) for PFVCN: 7.95–7.42 (m, 14H), 3.18 (br, 18H), 2.97 (br, 4H), 1.48 (br, 4H), 1.23–1.08 (br, 8H), 0.55 (br, 4H).

Characterization: ¹H NMR spectra were recorded on 300 MHz AC Bruker spectrometers. Mass spectra were measured by using an AEI M850-MS spectrometer. GPC analysis was carried out on a Waters Styragel system using polystyrene as the calibration standard and THF as eluent. UV-Vis absorption and fluorescence spectra were measured by using a Shimadzu UV-Vis spectrophotometer and a Jobin-Yvon Fluoromax-4 spectrofluorometer, respectively. Size distribution was measured by dynamic light scattering (DLS) (Zetasizer Nano ZS, Malvern). The fluorescence quantum yield of the polymers were measured by using fluorescein in aqueous solution (pH = 11) as the standard.

Two-Photon Excitation Fluorescence (TPEF) Measurements: TPEF measurements were performed by using a Avesta TiF-100M femtosecond (fs) Ti:sapphire oscillator as the excitation source. The output laser pulses have pulse duration of ~80 fs and a repetition rate of 84.5 MHz in the wavelength range from 750 to 850 nm. The laser beam was focused onto the sample that was contained in a cuvette with path length of 1 cm. The emission was collected at an angle of 90° to the incoming excitation beam by a pair of lenses and an optical fiber that was connected to a monochromator (Acton, Spectra Pro 2300i) coupled CCD (Princeton Instruments, Pixis 100B) system. A short pass filter with cutoff wavelength at 750 nm was placed before the spectrometer to minimize the scattering from the pump beam. Fluorescein in water (pH = 11), which have been well characterized in the literature,^[26] was used as reference (r). The two-photon absorption cross section of a sample can be calculated at each wavelength according to

$$\delta_s = \frac{S_s}{S_r} \cdot \frac{\phi_r}{\phi_s} \cdot \frac{C_r}{C_s} \cdot \delta_r \quad (1)$$

where S is the two-photon fluorescence signal, φ is the fluorescence quantum yield, and C is the concentration of the chromophore.^[6a] The concentration of the solution was in the range of 1 μM to 2 μM. The uncertainty in the measurement of cross sections is ~15%.

Detection of Singlet Oxygen: One-photon excitation singlet oxygen generation was directly monitored by the characteristic emission of singlet oxygen at ~1270 nm in CH₃OD solution. The singlet oxygen emission was measured by using a Fluorolog-3 iHR spectrofluorometer (Jobin-Yvon) equipped with a near-infrared sensitive photomultiplier (Hamamatsu model: R5509-72) operated at -80 °C. An 850 nm long-pass filter was placed before the detector. TMPyP₄ in D₂O was used as

the reference (r).^[3d] Singlet oxygen generation yield (Φ_Δ) of the sample under one-photon excitation can be calculated according to

$$\phi_{\Delta}^s = \phi_{\Delta}^r \cdot \frac{I_s}{I_r} \cdot \frac{A_r}{A_s} \cdot \frac{\tau_r}{\tau_s} \quad (2)$$

where I is the emission intensity of singlet oxygen at ~1270 nm, A is the absorbance of the solution. τ is the lifetime of singlet oxygen phosphorescence in selected solvent.^[27]

Two-photon excitation singlet oxygen generation was monitored by chemical oxidation of CHDDE in the aqueous solution. The sample solution was prepared by combing 1.0 mL of the polymer aqueous solution with CHDDE. The laser beam was focused onto a cuvette (1 cm path length) containing the sample solution. The decrease in the CHDDE absorbance was monitored under irradiation with fs laser pulses at 810 nm.

Cell Culture: The Hela cancer cells were cultured in growth media (DMEM supplemented with fetal bovine serum (10%), streptomycin (100.0 mg/L) and penicillin (100 IU/mL)). Cells were maintained in a humidified atmosphere of 5% CO₂ at 37 °C.

Proliferation Assay: Cell viability was determined by using the XTT colorimetric cell proliferation kit (Roche) following manufacturer's guidelines. Briefly, cells were grown to 20–30% confluence (since they will reach ~90% confluence with 24 h in the absence of compounds) in 96-well plates. The medium was aspirated and then treated with media (0.1 mL) containing different amounts of polymers or TMPyP₄. After incubation for 24 h, proliferation was assayed by using the XTT colorimetric cell proliferation kit (Roche). A total of three replicas were performed.

Two-Photon Cell Imaging: Hela cancer cells were seeded on glass-bottom dishes (Mattek) and grown until 70–80% confluence. The polymers or TMPyP₄ (0.5 μM) were added into the media and incubated for 3 h. After washing with the PBS buffer solution, DMEM media were added. The cancer cells were treated with PFV, PFVMO, PFVCN and TMPyP₄ for 3 h before the images were taken by using a Leica TCS SP5X confocal microscope system equipped with a water immersion objective (Leica HCX PL APO 63x/1.20 W CORR CS). A Ti-Sapphire oscillator at 810 nm was used as the two-photon excitation source. Images were processed by using Leica Application Suite Advanced Fluorescence (LAS AF) software.

Two-Photon Photodynamic Therapy Activity on Cancer Cells: Hela cancer cells were grown to 20–30% confluence in a 96-well plate. The medium was aspirated, washed with PBS, and then treated with media (0.1 mL) containing PFVCN or TMPyP₄. After incubation overnight in dark, cells were washed using PBS and re-cultured in a serum-containing DMEM medium. Each well was exposed to 1 kHz femtosecond laser irradiation at 810 nm with power density of ~3.0 W cm⁻². Cells after PDT treatments were further incubated for 24 h for apoptosis followed by the XTT assay of the cell proliferation. Cell experiments without nanoparticles under the same experimental conditions were performed for direct comparison.

Supporting Information

Supporting Information is available from the Wiley Online Library or from the author.

Acknowledgements

We thank the financial support from the Singapore-MIT Alliance of Research and Technology (SMART) program under National Research Foundation Singapore.

Received: November 1, 2012

- [1] a) D. E. J. G. Dolmans, D. Fukumura, R. K. Jain, *Nat. Rev. Cancer* **2003**, 3, 380; b) A. P. Castano, P. Mroz, M. R. Hamblin, *Nat. Rev. Cancer* **2006**, 6, 535; c) C. M. Moore, D. Pendse, M. Emberton, *Nat. Clin. Pract. Urol.* **2009**, 6, 18.
- [2] a) K. Ogawa, Y. Kobuke, *Anti-Cancer Agents Med. Chem.* **2008**, 8, 269; b) J. F. Lovell, T. W. B. Liu, J. Chen, G. Zheng, *Chem. Rev.* **2010**, 110, 2839.
- [3] a) N. L. Oleinick, R. L. Morris, I. Belichenko, *Photochem. Photobiol. Sci.* **2002**, 1, 1; b) T. C. Zhu, J. C. Finlay, *Med. Phys.* **2008**, 35, 3127; c) P. K. Frederiksen, M. Jorgensen, P. R. Ogilby, *J. Am. Chem. Soc.* **2001**, 123, 1215; d) P. K. Frederiksen, S. P. McIlroy, C. B. Nielsen, L. Nikolajsen, E. Skovsen, M. Jorgensen, K. V. Mikkelsen, P. R. Ogilby, *J. Am. Chem. Soc.* **2005**, 127, 255.
- [4] H. A. Collins, M. Khurana, E. H. Moriyama, A. Mariampillai, E. Dahlstedt, M. Balaz, M. K. Kuimova, M. Drobizhev, V. X. D. Yang, D. Phillips, A. Rebane, B. C. Wilson, H. L. Anderson, *Nat. Photonics* **2008**, 2, 420.
- [5] a) C. B. Nielsen, J. Arnbjerg, M. Johnsen, M. Jorgensen, P. R. Ogilby, *J. Org. Chem.* **2009**, 74, 9094; b) J. Arnbjerg, M. J. Paterson, C. B. Nielsen, M. Jorgensen, O. Christiansen, P. R. Ogilby, *J. Phys. Chem. A* **2007**, 111, 5756; c) M. Velusamy, J. Y. Shen, J. T. Lin, Y. C. Lin, C. C. Hsieh, C. H. Lai, C. W. Lai, M. L. Ho, Y. C. Chen, P. T. Chou, J. K. Hsiao, *Adv. Funct. Mater.* **2009**, 19, 2388; d) M. K. Kuimova, H. A. Collins, M. Balaz, E. Dahlstedt, J. A. Levitt, N. Sergeant, K. Suhling, M. Drobizhev, N. S. Makarov, A. Rebane, H. L. Anderson, D. Phillips, *Org. Biomol. Chem.* **2009**, 7, 889; e) M. Balaz, H. A. Collins, E. Dahlstedt, H. L. Anderson, *Org. Biomol. Chem.* **2009**, 7, 874.
- [6] a) Y. Tian, C. Y. Chen, Y. J. Cheng, A. C. Young, N. M. Tucker, A. K. Y. Jen, *Adv. Funct. Mater.* **2007**, 17, 1691; b) W. R. Dichtel, J. M. Serin, C. Edler, J. M. J. Frechet, M. Matuszewski, L. S. Tan, T. Y. Ohulchanskyy, P. N. Prasad, *J. Am. Chem. Soc.* **2004**, 126, 5380; c) R. P. Brinas, T. Troxler, R. M. Hochstrasser, S. A. Vinogradov, *J. Am. Chem. Soc.* **2005**, 127, 11851; d) C. Y. Chen, Y. Q. Tian, Y. J. Cheng, A. C. Young, J. W. Ka, A. K. Y. Jen, *J. Am. Chem. Soc.* **2007**, 129, 7220; e) S. Kim, T. Y. Ohulchanskyy, H. E. Pudavar, R. K. Pandey, P. N. Prasad, *J. Am. Chem. Soc.* **2007**, 129, 2669.
- [7] J. P. Celli, B. Q. Spring, I. Rizvi, C. L. Evans, K. S. Samkoe, S. Verma, B. W. Pogue, T. Hasan, *Chem. Rev.* **2010**, 110, 2795.
- [8] a) M. Loning, H. Diddens, W. Kupker, K. Diedrich, G. Huttman, *Cancer* **2004**, 100, 1650; b) P. Redondo, M. Marquina, M. Pretel, L. Aguado, M. E. Iglesias, *Arch. Dermatol.* **2008**, 144, 115; c) W. Zhong, J. P. Celli, I. Rizvi, Z. Mai, B. Q. Spring, S. H. Yun, T. Hasan, *Brit. J. Cancer* **2009**, 101, 2015.
- [9] a) W. R. Zipfel, R. M. Williams, W. W. Webb, *Nat. Biotechnol.* **2003**, 21, 1368; b) F. Helmchen, W. Denk, *Nat. Methods* **2005**, 2, 932.
- [10] X. Shen, L. Li, H. Wu, S. Q. Yao, Q.-H. Xu, *Nanoscale* **2011**, 3, 5140.
- [11] a) S. W. Thomas, G. D. Joly, T. M. Swager, *Chem. Rev.* **2007**, 107, 1339; b) C. F. Wu, C. Szymanski, Z. Cain, J. McNeill, *J. Am. Chem. Soc.* **2007**, 129, 12904; c) C. L. Zhu, L. B. Liu, Q. Yang, F. T. Lv, S. Wang, *Chem. Rev.* **2012**, 112, 4687.
- [12] a) N. Tian, Q. H. Xu, *Adv. Mater.* **2007**, 19, 1988; b) C. L. Wu, Q. H. Xu, *Macromol. Rapid Commun.* **2009**, 30, 504; c) F. He, X. Ren, X. Shen, Q.-H. Xu, *Macromolecules* **2011**, 44, 5373.
- [13] X. Q. Shen, F. He, J. H. Wu, G. Q. Xu, S. Q. Yao, Q. H. Xu, *Langmuir* **2011**, 27, 1739.
- [14] a) C. F. Wu, C. Szymanski, Z. Cain, J. McNeill, *J. Am. Chem. Soc.* **2007**, 129, 12904; b) K. S. Schanze, A. Parthasarathy, H. Y. Ahn, K. D. Belfield, *ACS Appl. Mater. Inter.* **2010**, 2, 2744; c) N. A. A. Rahim, W. McDaniel, K. Bardion, S. Srinivasan, V. Vickerman, P. T. C. So, J. H. Moon, *Adv. Mater.* **2009**, 21, 3492.
- [15] a) L. D. Lu, F. H. Rininsland, S. K. Wittenburg, K. E. Achyuthan, D. W. McBranch, D. G. Whitten, *Langmuir* **2005**, 21, 10154; b) S. Chemburu, T. S. Corbitt, L. K. Ista, E. Ji, J. Fulghum, G. P. Lopez, K. Ogawa, K. S. Schanze, D. G. Whitten, *Langmuir* **2008**, 24, 11053; c) T. S. Corbitt, L. P. Ding, E. Y. Ji, L. K. Ista, K. Ogawa, G. P. Lopez, K. S. Schanze, D. G. Whitten, *Photochem. Photobiol. Sci.* **2009**, 8, 998; d) E. Ji, T. S. Corbitt, A. Parthasarathy, K. S. Schanzes, D. G. Whitten, *ACS Appl. Mater. Inter.* **2011**, 3, 2820.
- [16] a) H. Chong, C. Y. Nie, C. L. Zhu, Q. Yang, L. B. Liu, F. T. Lv, S. Wang, *Langmuir* **2012**, 28, 2091; b) X. Duan, L. Liu, X. Feng, S. Wang, *Adv. Mater.* **2010**, 22, 1.
- [17] a) S. J. K. Pond, M. Rumi, M. D. Levin, T. C. Parker, D. Beljonne, M. W. Day, J. L. Bredas, S. R. Marder, J. W. Perry, *J. Phys. Chem. A* **2002**, 106, 11470; b) S. K. Lee, W. J. Yang, J. J. Choi, C. H. Kim, S. J. Jeon, B. R. Cho, *Org. Lett.* **2005**, 7, 323.
- [18] a) H. A. Ho, M. Leclerc, *J. Am. Chem. Soc.* **2004**, 126, 1384; b) X. Y. Zhao, M. R. Pinto, L. M. Hardison, J. Mwaura, J. Muller, H. Jiang, D. Witker, V. D. Kleiman, J. R. Reynolds, K. S. Schanze, *Macromolecules* **2006**, 39, 6355; c) M. Fakis, D. Anastopoulos, V. Giannetas, P. Persephonis, J. Mikroyannidis, *J. Phys. Chem. B* **2006**, 110, 12926; d) T. Q. Nguyen, V. Doan, B. J. Schwartz, *J. Chem. Phys.* **1999**, 110, 4068.
- [19] a) C. Tan, M. R. Pinto, K. S. Schanze, *Chem. Commun.* **2002**, 446; b) B. J. Schwartz, *Annu. Rev. Phys. Chem.* **2003**, 54, 141.
- [20] J. B. Birks, *Rep. Prog. Phys.* **1975**, 38, 903.
- [21] a) X. L. Feng, Y. L. Tang, X. R. Duan, L. B. Liu, S. Wang, *J. Mater. Chem.* **2010**, 20, 1312; b) C. Wu, B. Bull, C. Szymanski, K. Christensen, J. McNeill, *ACS Nano* **2008**, 2, 2415.
- [22] a) Z. Fang, X. H. Zhang, Y. H. Lai, B. Liu, *Chem. Commun.* **2009**, 920; b) S. Kim, Q. Zheng, G. S. He, D. J. Bharali, H. E. Pudavar, A. Baev, P. N. Prasad, *Adv. Funct. Mater.* **2006**, 16, 2317.
- [23] a) H. Y. Woo, J. W. Hong, B. Liu, A. Mikhailovsky, D. Korystov, G. C. Bazan, *J. Am. Chem. Soc.* **2005**, 127, 820; b) H. Y. Woo, D. Korystov, A. Mikhailovsky, T. Q. Nguyen, G. C. Bazan, *J. Am. Chem. Soc.* **2005**, 127, 13794.
- [24] V. Nardello, N. Azaroual, I. Cervoise, G. Vermeersch, J. M. Aubry, *Tetrahedron* **1996**, 52, 2031.
- [25] a) J. K. Lee, R. R. Schrock, D. R. Baigent, R. H. Friend, *Macromolecules* **1995**, 28, 1966; b) J. Eldo, A. Ajayaghosh, *Chem. Mater.* **2002**, 14, 410.
- [26] C. Xu, W. W. Webb, *J. Opt. Soc. Am. B* **1996**, 13, 481.
- [27] C. Tanielian, G. Heinrich, *Photochem. Photobiol.* **1995**, 61, 131.